A Tightly Combined GPS/Galileo Model for Long Baseline RTK Positioning with Partial Ambiguity Resolution

Qing Zhao, Chengfa Gao, Shuguo Pan, Ruicheng Zhang
and Liwei Liu

Abstract Knowledge of differential inter-system biases (DISBs) is critical to integrate observations from mixed GNSS. If the corresponding DISB could be calibrated in advance, only one pivot satellite is sufficient for ambiguity resolution on overlapping frequencies, which is the so-called tight combining (TC) strategy. Considering that GPS and Galileo transmit signals on two identical frequencies (e.g. L1/E1 and L5/E5a), a tightly combined GPS/Galileo RTK positioning model is proposed in this paper. Traditional DD model has been slightly adjusted to avoid the hand-over problem of reference satellites. The estimation of code and fractional part of phase DISB is archived through zero and ultra-short baselines. Three long baselines were selected to verify the proposed model with DISB calibrated in advance. Moreover, to get better AR performance, a simple but robust procedure of PAR, where the satellite elevation, number of consecutive tracking, success rate and ratio test are all combined to determine the subset of ambiguity, is adopted in the long baseline experiments. Results shows that the code and fractional part of phase DISB is rather stable. The TC strategy do not significantly improve the value of ratio, but shorten the convergence time to reach the 100% success rate. Compared with results of loose combining (LC) strategy, time to first fix (TTFF) is further reduced by 54.3, 72.9, 69.0% respectively under TC strategy corresponding to different long baselines. Besides, TC strategy could slightly improve the fixing rate of epochs. In terms of accuracy, the precision in up direction is worse than that in north and east direction. Once the ambiguity is fixed correctly, both LC and TC strategy can achieve centimeter-level positioning accuracy.

Q. Zhao · C. Gao (✉) · R. Zhang
School of Transportation, Southeast University, 2 Sipailou,
Nanjing 210096, China
e-mail: 230169553@seu.edu.cn

S. Pan (✉) · L. Liu
School of Instrument Science and Engineering, Southeast University,
2 Sipailou, Nanjing 210096, China
e-mail: psg@seu.edu.cn

673

1 Introduction

Today, the Global Navigation Satellite System (GNSS) has been widely used for a multitude of applications around the world. Multi-GNSS differential positioning requires different reference satellite for each system, which is referred to as loose combining (LC) [1], and the performance of BDS/GPS dual/triple frequency was investigated by Gao et al. [2, 3]. On the other hand, combining observations on same frequencies from multi-GNSS in one positioning model with a common pivot satellite, which is the so-called tight combining (TC) [4], can introduce at least one more redundancy and will be beneficial to ambiguity resolution (AR) performance which is essential to high-precision mixed-constellation RTK positioning. The performance in terms of accuracy, availability and reliability of GPS only is largely a function of the number of satellite being tracked. Thus, the GPS real-time kinematic (RTK) positioning solution is degraded in urban canyon environment or in deep open cut mines where the number of visible satellite is limited [5]. The Galileo in EU is a one of the aiding solutions to add more functioning satellites which shares two overlapping frequencies (e.g. L1/E1 and L5/E5a) with GPS [6]. However, proper handling of the GNSS hardware biases known as differential inter-system bias (DISB) [7] is the prerequisite for integrating GPS and Galileo in one rigorous model. Studies on DISB have become the focus in the GNSS community. The GPS-Galileo ISB was first carried out by Montenbruck in CONGO network experiment [8]. Odijk and Teunissen pointed out that the range ISB can be estimated along with the coordinate parameters, while the phase ISB can be lump together with ambiguity parameters [9], however, this will not do any impact on the positioning results. A particle filter-based method for estimation of ISB was proposed by Tian et al. [10]. In addition to identical frequencies, DISB model between GPS and BDS on different frequencies was also studied and verified by Gao et al. [11].

Correct estimates of the carrier phase integer ambiguities are the prerequisite for high-precision positioning, since incorrect ambiguity fixing can lead to largely biased positioning solutions. However, it is not easy to fix all ambiguities simultaneously. In such cases, it may be beneficial to consider partial ambiguity resolution (PAR) techniques, which resolve only a subset of ambiguities. The important thing is how to determine the subset. Choice of an ambiguity subset could be based on ambiguity variance, pre-defined subset sizes, elevation ordering and linear combinations [12]. Parkins proposed a PAR method to deal with the presence of biased observations [13], but it is very time-consuming. An elevation-based technique was applied to the GPS/BDS/GLONASS RTK positioning by Gao et al. [14]. Unlike the usual method, a modified partial ambiguity resolution procedure is proposed by Wang and Feng [15], where the indices of both the success rate and the ratio test are combined to find an optimal ambiguity subset to be fixed. It was

widely demonstrated that the PAR strategy could obviously shorten the time to reach centimeter level accuracy for long baselines, and considerably extend the range for instantaneous RTK positioning [16].

Although many studies have been focused on the DISB with zero/ultra-short or medium-baseline experiments, the effect of application under long baseline conditions remains to be further studied. Therefore, this paper aims to make a preliminary assessment of the DISB application in the case of long baseline. In the following, Sect. 2 details the mathematical derivations of TC observation model, DISB estimation model and PAR procedure; Sect. 3 presents the data and models used in the experiments; Sect. 4 analysis the results of estimated DISB, performance of AR and positioning accuracy; finally, Sect. 5 summarizes the main point of this paper.

2 Methods

2.1 Intra-system and Inter-system Observation Model

For GPS and Galileo, the discrepancy in coordinate and time systems may be negligible in most applications. They transmitted signals on identical frequencies of L1/E1 and L5/E5a, which enables only one common pivot satellite once the DISB is calibrated. For long baselines, the differential atmospheric delays between receivers need to be considered. The between-receiver SD observation equations for GPS or Galileo can be expressed as

$$
\begin{aligned}
\Delta L_{r_1 r_2}^S &= \Delta \rho_{r_1 r_2}^S + \Delta dt_{r_1 r_2} + \Delta T_{r_1 r_2}^S - \mu \cdot \Delta I_{r_1 r_2}^S + \lambda \cdot \Delta N_{r_1 r_2}^S + b_{r_1 r_2}^S \\
\Delta P_{r_1 r_2}^S &= \Delta \rho_{r_1 r_2}^S + \Delta dt_{r_1 r_2} + \Delta T_{r_1 r_2}^S + \mu \cdot \Delta I_{r_1 r_2}^S + B_{r_1 r_2}^S
\end{aligned}
\tag{1}
$$

where, Δ is the between-receiver SD operator; L is the carrier observation and P is pseudorange observation; The superscript S represents the satellite of GPS or Galileo and the subscript r represents different receivers; ρ is the distance between satellite and receiver; dt denotes the receiver clock error; λ denotes the wavelength; b denotes the hardware phase delay, which also contains the initial phase in the receiver; N denotes the integer phase ambiguity; T denotes the tropospheric delay, and I denotes the ionospheric delay; μ is the ionospheric scale factor; B denotes the hardware code delay in the receiver for GPS or Galileo.

Based on SD observation equations, the classical intra-system DD observation can be formed, where the receiver-dependent bias can be eliminated. Here, we choose G_1 as the reference satellite for GPS and E_1 for Galileo, we can obtain

$$\nabla\Delta L_{r_1 r_2}^{G_1 G_s} = \nabla\Delta\rho_{r_1 r_2}^{G_1 G_s} + \nabla\Delta T_{r_1 r_2}^{G_1 G_s} - \mu \cdot \nabla\Delta I_{r_1 r_2}^{G_1 G_s} + \lambda \cdot \nabla\Delta N_{r_1 r_2}^{G_1 G_s}$$

$$\nabla\Delta P_{r_1 r_2}^{G_1 G_s} = \nabla\Delta\rho_{r_1 r_2}^{G_1 G_s} + \nabla\Delta T_{r_1 r_2}^{G_1 G_s} + \mu \cdot \nabla\Delta I_{r_1 r_2}^{G_1 G_s}$$

$$\nabla\Delta L_{r_1 r_2}^{E_1 E_s} = \nabla\Delta\rho_{r_1 r_2}^{E_1 E_s} + \nabla\Delta T_{r_1 r_2}^{E_1 E_s} - \mu \cdot \nabla\Delta I_{r_1 r_2}^{E_1 E_s} + \lambda \cdot \nabla\Delta N_{r_1 r_2}^{E_1 E_s}$$

$$\nabla\Delta P_{r_1 r_2}^{E_1 E_s} = \nabla\Delta\rho_{r_1 r_2}^{E_1 E_s} + \nabla\Delta T_{r_1 r_2}^{E_1 E_s} + \mu \cdot \nabla\Delta I_{r_1 r_2}^{E_1 E_s}$$

$$(2)$$

where, $\nabla\Delta$ is the double-differential operator; G and E represents satellites of GPS and Galileo respectively. The meaning of other characters is as described above.

The inter-system DD observation equations between GPS and Galileo on same frequencies can also be built in a similar way, but the hardware delays cannot be eliminated. The corresponding models can be expressed as

$$\nabla\Delta L_{r_1 r_2}^{G_1 E_s} = \nabla\Delta\rho_{r_1 r_2}^{G_1 E_s} + \nabla\Delta T_{r_1 r_2}^{G_1 E_s} - \nabla\Delta I_{r_1 r_2}^{G_1 E_s} + \lambda \cdot \nabla\Delta N_{r_1 r_2}^{G_1 E_s} + \nabla\Delta b_{r_1 r_2}^{GE}$$

$$\nabla\Delta P_{r_1 r_2}^{G_1 E_s} = \nabla\Delta\rho_{r_1 r_2}^{G_1 E_s} + \nabla\Delta T_{r_1 r_2}^{G_1 E_s} + \nabla\Delta I_{r_1 r_2}^{G_1 E_s} + \nabla\Delta B_{r_1 r_2}^{GE}$$

$$(3)$$

where, $\nabla\Delta b_{r_1 r_2}^{GE}$ and $\nabla\Delta B_{r_1 r_2}^{GE}$ represent the phase and code DISB between GPS and Galileo on overlapping frequencies. Odijk and Teunissen [7] and Paziewski et al. [6] have studied the DISB on same frequencies and demonstrated that the DISB is rather stable in time and related to the receiver type and signal frequency. Therefore carrier phase and code ISBs for a particular receiver pair can be estimated once and introduced as a known correction in GPS/Galileo tightly combined processing.

In order to avoid the hand-over problem of reference satellites in traditional DD model, we made some adjustments where the estimated DD tropospheric delay is expressed in the form of zero-differenced and the estimated DD ionospheric delay, DD ambiguities are all maintain the form of between-receiver single difference.

$$\nabla\Delta L_{r_1 r_2}^{G_1 E_s} - \nabla\Delta b_{r_1 r_2}^{GE} = \nabla\Delta\rho_{r_1 r_2}^{G_1 E_s} + \left(M_{r_2}^{E_s} - M_{r_2}^{G_1}\right)T_{r_2} - \left(M_{r_1}^{E_s} - M_{r_1}^{G_1}\right)T_{r_1} - \mu \cdot \left(\Delta I_{r_1 r_2}^{E_s} - \Delta I_{r_1 r_2}^{G_1}\right)$$
$$+ \lambda \cdot \left(\Delta N_{r_1 r_2}^{E_s} - \Delta N_{r_1 r_2}^{G_1}\right)$$

$$\nabla\Delta P_{r_1 r_2}^{G_1 E_s} - \nabla\Delta B_{r_1 r_2}^{GE} = \nabla\Delta\rho_{r_1 r_2}^{G_1 E_s} + \left(M_{r_2}^{E_s} - M_{r_2}^{G_1}\right)T_{r_2} - \left(M_{r_1}^{E_s} - M_{r_1}^{G_1}\right)T_{r_1} + \mu \cdot \left(\Delta I_{r_1 r_2}^{E_s} - \Delta I_{r_1 r_2}^{G_1}\right)$$

$$(4)$$

where M is the mapping function of tropospheric delay, here the niell mapping function is used.

After making the above adjustments to the model, the unknown state x vector is defined as:

$$x = \left(X, Y, Z, T_{r_2}, T_{r_1}, I_1, I_2, \ldots, I_{Maxsat}, N_1, N_2, \ldots, N_{Maxsat \cdot numfreq}\right) \qquad (5)$$

where, *Maxsat* and *numfreq* represents the number of satellites and frequencies respectively.

2.2   Estimation of DISB

The phase and code ISBs can be estimated precisely on zero or ultra-short baselines based on Eq. (3) where differential atmosphere errors could be ignored. Due to the integer part of DISB is linearly dependent with ambiguity so they can be lumped together, so we could only get the fractional part of the phase DISB. Of course, this rank deficiency problem do not exist in the estimation of code DISB. The code and fractional part of phase DISB can be calculated through the following equation,

$$
\begin{aligned}
\nabla\Delta b^{GE}_{r_1r_2,fractional} &= \left(\nabla\Delta L^{G_1E_s}_{r_1r_2} - \nabla\Delta\rho^{G_1E_s}_{r_1r_2}\right)/\lambda - \left[\left(\nabla\Delta L^{G_1E_s}_{r_1r_2} - \nabla\Delta\rho^{G_1E_s}_{r_1r_2}\right)/\lambda\right] \\
\nabla\Delta B^{GE}_{r_1r_2} &= \nabla\Delta P^{G_1E_s}_{r_1r_2} - \nabla\Delta\rho^{G_1E_s}_{r_1r_2}
\end{aligned}
\tag{6}
$$

where, the $[\cdot]$ denotes rounding function.

2.3   Strategy of Partial Ambiguity Resolution

In the multi-constellation RTK processing, it is not easy to fix all ambiguities reliably, however, one could have sufficient confidence to fix a subset of the ambiguities, which is referred to as partial ambiguity resolution (PAR) [17]. As we all know, the low-elevation ambiguities suffer much more from observation noise, multipath effects and the residual atmospheric delays, and thus have lower accuracies and also take longer to converge to a certain degree of precision. Therefore it is generally hard to fix these ambiguities correctly due to its poor accuracy and high correlation with others. In the other hand, if we fix all the ambiguities simultaneously, the low-elevation ones may influence the search system and make the search result unable to pass the acceptance test [14]. Fortunately, the number of visible satellites greatly increases when both GPS and Galileo are used, which means a higher cut-off angle could be used. In this Section, a simple but robust PAR strategy with ambiguity subset selected based on the elevations and the number of consecutive tracking will be introduced. Figure 1 presents the flowchart of this procedure.

First, the procedure starts with SD float ambiguity and an initial elevation mask of 10 degrees, and the threshold number of consecutive locked is set to 10, then we could get the DD float solution and the corresponding variance. If the number of DD float ambiguity is greater than 6, the LAMBDA method is applied to get the optimal candidate. If the bootstrapping success rate and value of ratio is higher than the threshold (e.g., 0.99 and 3.0), tight constraints is applied on ambiguities which is the so-called "Fix and Hold", and the ambiguity-fixed solution is achieved. Otherwise, the elevation mask of AR will increase by 5°, and repeat the LAMBDA search and AR test. Until the number of DD ambiguities is less than 6, the iteration will be terminated and only a float solution is achieved at this epoch.
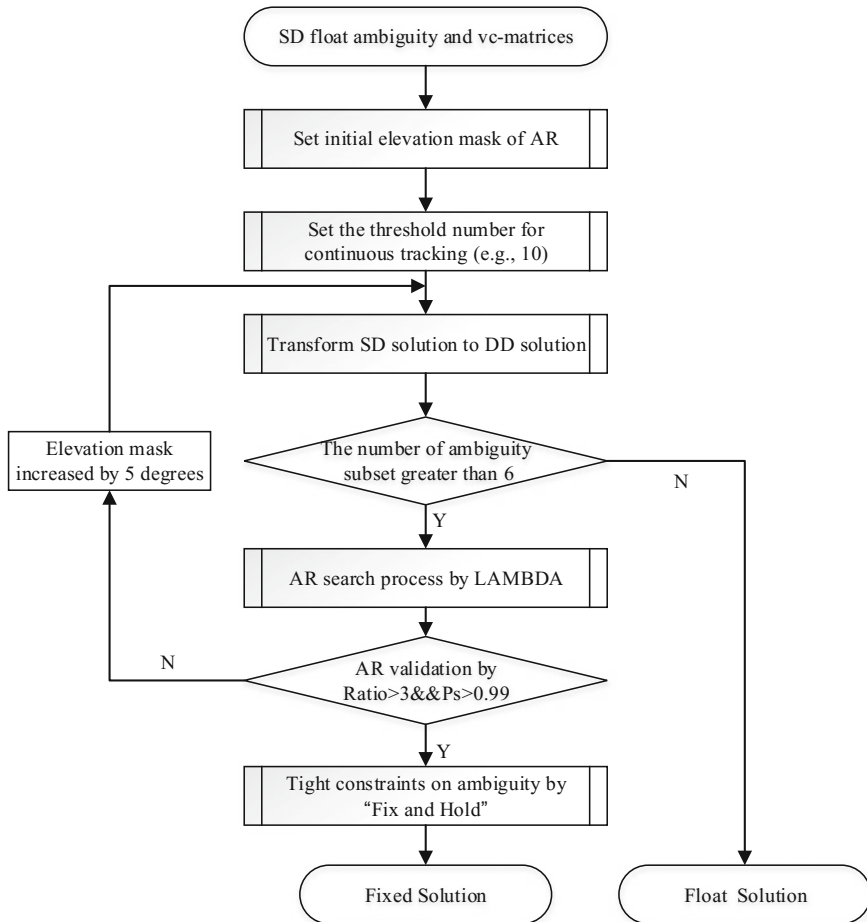
Fig. 1 The flowchart of PAR procedure

3 Data Processing

Similar to earlier DISB studies, the estimation of code and phase DISBs on overlapping frequencies L1/E1 and L5/E5a is achieved through zero and ultra-short baselines, since the atmospheric effects can be ignored. Here, three MGEX stations (CUT0, CUT2, CUTC) in campus of Curtin University, Australia is selected. As mentioned earlier, the purpose of DISB calibration is to improve the performance of ambiguity resolution which is essential to high-precision mixed-constellation RTK positioning. The calibration of DISB is verified with 3 long baselines range from 570 to 1200 km which is formed by PERT, MRO1 and KARR in Australia. It is worth mentioning that the coordinates of the MGEX stations are known and have

Table 1 Baselines used in the experiment of estimation and calibration of DISB

Baseline	Receiver Type1 (Version)	Receiver Type2 (Version)	Baseline Length	Remark
CUT2-CUT0	Trimble NETR9 (5.22)	Trimble NETR9 (5.22)	0 m	Estimation
CUTC-CUT0	Trimble NETR9 (5.30)	Trimble NETR9 (5.22)	8 m	
MRO1-KARR	Trimble NETR9 (5.22)	Trimble NETR9 (5.22)	634.484 km	Calibration
PERT-MRO1	Trimble NETR9 (5.30)	Trimble NETR9 (5.22)	570.399 km	
PERT-KARR	Trimble NETR9 (5.30)	Trimble NETR9 (5.22)	1203.129 km	

an accuracy of a few millimeters. Detailed information for each baseline is shown in Table 1. All stations are equipped with Trimble NETR9 receiver but different firmware version. The data were collected on DOY 300, 2017 with the sampling interval of 30 s.

Table 2 summarizes the detailed processing strategy for long baseline RTK positioning. Precise orbit at intervals 5 min provided by MGEX (e.g., GFZ) were used since the accuracy of broadcast ephemeris is limited. For data modeling, we applied the absolute phase centers [18], the phase-wind up effects [19] and the station displacement models proposed by IERS Convensions 2010 [20]. A cut-off angel of 10° was set for usable measurement and an elevation-dependent weighting strategy was applied to measurements where a priori precision of 3 mm and 3 m for raw phase and code, respectively. In addition, the station coordinate was estimated as white noise process with variance of 30^2 m^2. The bootstrapping success rate and ratio-test threshold were 0.99 and 3.0 respectively.

4 Results and Discussion

In this section, we first discuss the characteristics of the code/phase DISB estimated from zero or ultra-short baseline, then analysis the ambiguity performance of long baseline RTK positioning with DISB calibration, and finally address the statistical results of positioning accuracy under LC and TC strategy.

4.1 Results of Code/Phase DISB

The estimated code and phase DISB on frequencies L1/E1 and L5/E5a calculated from Eq. (6) are shown in Figs. 2 and 3 respectively. It is obviously that the DISB

Table 2 Tightly combined processing strategy for long baseline

Item	Models
Solution mode	Kinematic
Constellation	GPS & Galileo
Observations	Carrier phase and code observations
Estimator	Kalman filter
Frequency selection	GPS:L1/L2/L5; Galileo:E1/E5a/E5b
Elevation cutoff angle	10°
Sampling rate	30 s
Weighting scheme	Elevation-dependent weight: A priori precision of 3 mm and 3 m for raw phase and code, respectively
Ionospheric delay	Estimated as random-walk process
Tropospheric delay	Dry component: corrected with standard atmosphere and Saastamoinen model Wet component: estimated as random-walk process(10^{-8} m^2/s), NMF mapping function applied
Sagnac effect	Applied
Station displacement	Corrected by IERS Convention 2010
Satellite antenna PCO/PCV	Corrected by IGS 14.atx
Receiver antenna PCO/PCV	PCO/PCV values for GPS from IGS14.atx are used
Satellite orbit	Fixed to MGEX (GFZ) products
Satellite clock	DD eliminated or weakening
Receiver clock	DD eliminated or weakening
Station coordinate	Estimated as white noise process (30^2 m^2)
Phase ambiguity	Estimated, constant for each continuous arcs, Fix and Hold
Bootstrapping success rate threshold	0.99
Ratio test threshold	3.0

is rather stable over the whole observation period regardless of the random terms caused by observation noises. The mean of phase DISB over the day is close to zero indeed and the standard deviations for both L1/E1 and L5/E5a are all within 0.02 cycles. Compared with phase DISB, the code DISB show greater noise due to the pseudorange noise and the standard deviations are all within 0.6 m. Despite the larger noise in code DISB, the amplitude is still relatively stable. The detailed statistical results is summarized in Table 3.

It can be seen that the code and phase DISB on both frequencies estimated from CUTC-CUT0 show larger noise than that from CUT2-CUT0. This may be caused by the following two reasons: The first one is that the different firmware version over the both sides of the baseline CUTC-CUT0; The second is that the baseline CUT2-CUT0 is a zero baseline for which differential atmospheric errors are completely absent and multi-path errors are very minor while the baseline CUTC-CUT0
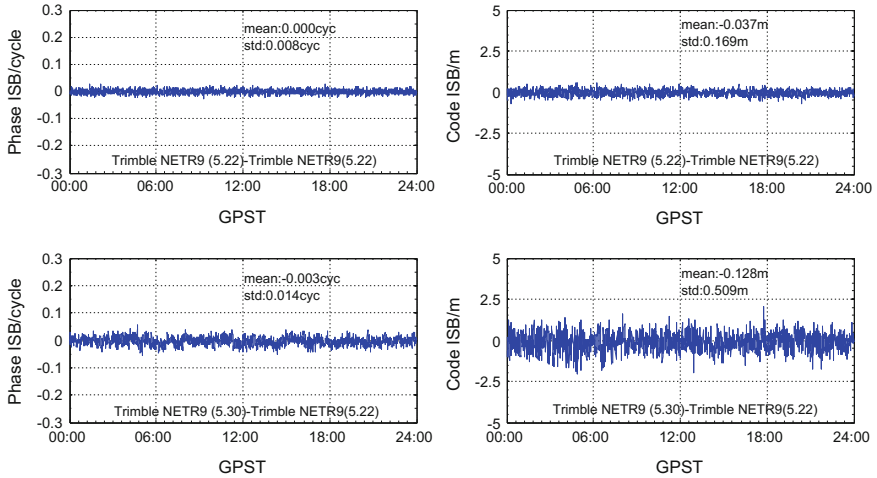
Fig. 2 Estimated fractional phase (left) and code (right) DISB on L1/E1 corresponding to CUT2-CUT0 (top) and CUTC-CUT0 (bottom)
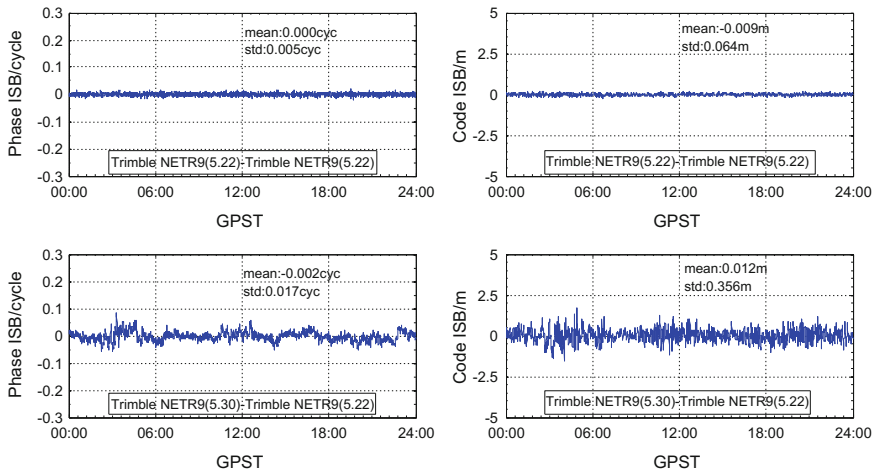

Fig. 3 Estimated fractional phase (left) and code (right) DISB on L5/E5a corresponding to CUT2-CUT0 (top) and CUTC-CUT0 (bottom)

Table 3 Statistical results of fractional phase and code DISB

Baseline	L1/E1 Phase		L1/E1 Code		L5/E5a Phase		L5/E5a Code	
	Mean/cyc	Std/cyc	Mean/m	Std/m	Mean/cyc	Std/cyc	Mean/m	Std/m
CUT2-CUT0	0.000	0.008	−0.037	0.169	0.000	0.005	−0.009	0.064
CUTC-CUT0	−0.003	0.014	−0.128	0.509	−0.002	0.017	0.012	0.356

is a nonzero-baseline. We adopted the DISB calibration in the long baseline experiments corresponding to the receiver firmware version.

4.2   Results of AR Performance

The AR results of LC and TC for three different long baselines are shown in this section. Figure 4 shows the value of ratio (left) over the day and success rate (right) for the first 6 h. From Fig. 4, we can find that TC strategy do not significantly improve the value of ratio, but shorten the convergence time to reach the 100% success rate. This is because that during the initial period, TC strategy could provide more observations, so additional redundancies are introduced which is beneficial to the ambiguity resolution.

Figure 5 shows the AR performance in terms of TTFF (left) and the fixing rate (right) of three different long baselines under LC and TC strategy. In this paper, the TTFF was defined as the time taken for the ambiguity-fixed solution to be successfully achieved and the following 10 epochs also keep fixed. The fixing rate was defined as the ratio of the number of fixed epochs to the number of total epochs during this period. Since we apply the DISB calibration advance in TC strategy,
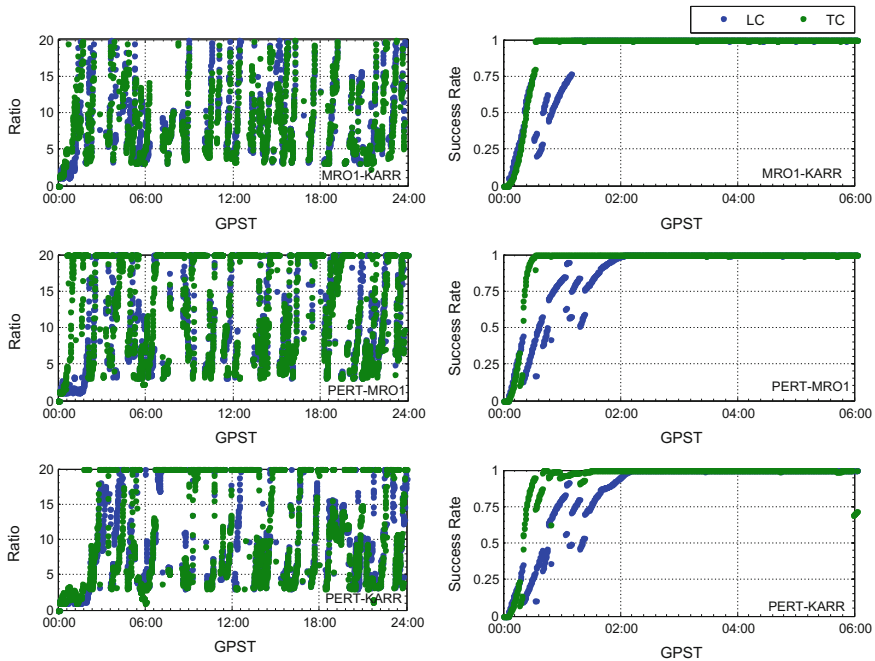

Fig. 4 Ratio value (left) and bootstrapping success rate (right) corresponding to MRO1-KARR (top), PERT-MRO1 (medium), PERT-KARR (bottom) under LC and TC strategy respectively
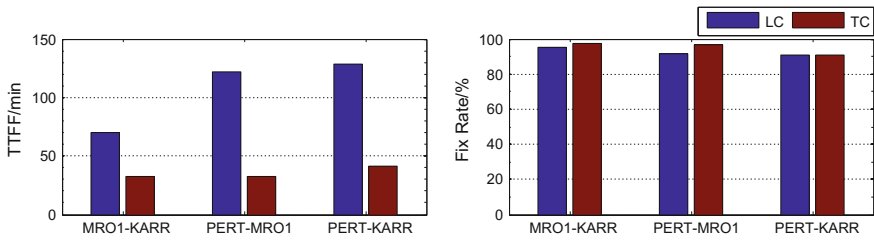
Fig. 5 TTFF (left) and fix rate (right) of epochs correspond to different baselines

there is more redundancies compared with LC strategy, which result in shorter convergence time to first fix, as shown in Fig. 5. The time to first fix is 70, 122, 129 min under LC strategy, while only 32, 33, 40 min under TC strategy corresponding to MRO1-KARR, PERT-MRO1, PERT-KARR baseline. Compared with results of LC strategy, TTFF is further reduced by 54.3, 72.9, 69.0% respectively. Figure 5 (right) also shows that TC strategy could slightly improve the fixing rate of epochs.

Figure 6 shows the common view satellite number of Galileo (top) and ambiguity fix period of Galileo (bottom) corresponding to MRO1-KARR baseline. It is easy to find that TC could achieve longer fixing period. During some period as checked in red rectangle in Fig. 6, there is only one common view Galileo satellite
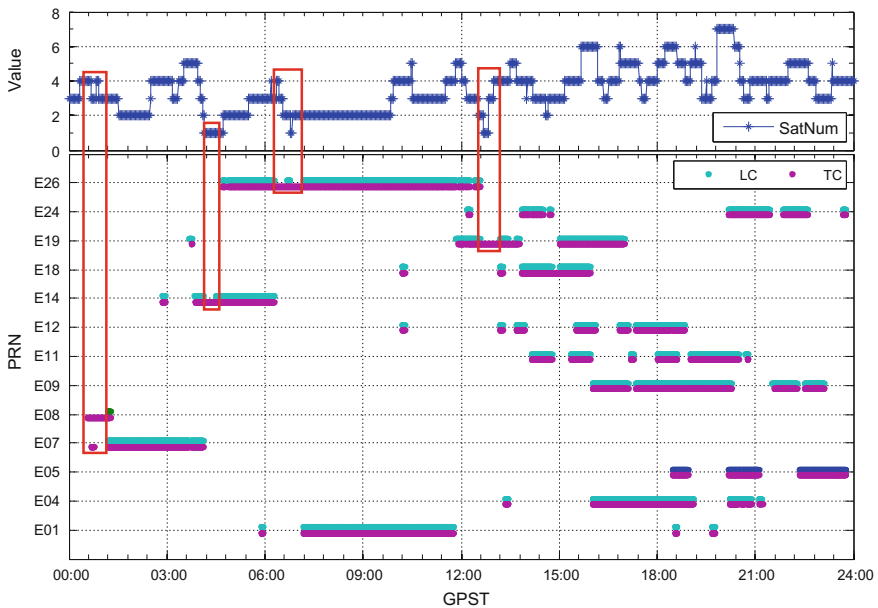

Fig. 6 Common view satellite number (top) and fixed period (bottom) of Galileo system corresponding to MRO1-KARR

where double-difference ambiguity could not be formed within Galileo system and the number of satellites is dramatically changing which lead to frequent reinitialization of new rise satellites, LC could only keep float solutions, while TC could still get the fixed solutions. It come to the following conclusion that compared with LC strategy, TC strategy has a better performance in AR.

4.3   Results of Positioning

As mentioned earlier, the coordinates of three stations are precisely known from the IGS weekly solution. Baseline errors are the difference between the estimated baseline length and precise reference baseline length. Baseline errors of different combination strategy are shown in Fig. 7. The light green dotted line in the figure marked the TTFF. It is easy to find that fluctuation in the up direction is larger than that in north and east direction. Detailed precision statistics are summarized in
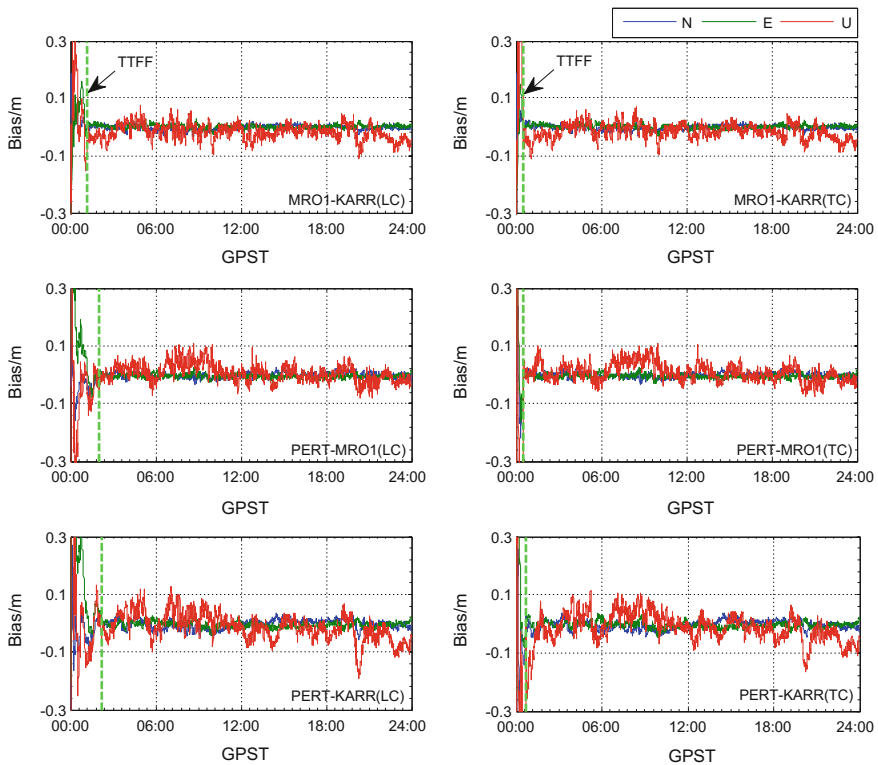
Fig. 7 Baseline errors for LC (left) and TC (right) strategy corresponding to MRO1-KARR (top), PERT-MRO1 (medium), PERT-KARR (bottom)

Table 4 RMS statistics of baseline error

Baseline	LC-RMS				TC-RMS			
	N/m	E/m	U/m	3D/m	N/m	E/m	U/m	3D/m
MRO1-KARR	0.009	0.007	0.032	0.034	0.008	0.007	0.031	0.033
PERT-MRO1	0.009	0.009	0.030	0.033	0.009	0.009	0.031	0.034
PERT-KARR	0.016	0.011	0.048	0.052	0.015	0.011	0.046	0.050

Table 4. It must be noted that only the ambiguity-fixed solution is contained in the statistics. The 3D positioning errors is 3.4, 3.3, 4.8 cm under LC strategy, while 3.3, 3.4, 5.0 cm under TC strategy corresponding to MRO1-KARR, PERT-MRO1, PERT-KARR baseline. LC and TC strategy could both achieve centimeter-level positioning accuracy in the case of ambiguity fixed correctly. The length of PERT-KARR is almost twice of that of other two baselines and the accuracy of PERT-KARR baseline is also worse than that of other two baselines due to residual atmospheric errors, such as residual tropospheric delay and ionospheric delay.

5 Conclusions

We first propose a GPS/Galileo tightly combined RTK positioning model with raw carrier phase and code observations for long baselines which avoid the hand-over problem of reference satellites in traditional DD model, then the estimation of DISB model based on zero or ultra-short baseline is developed. In order to get better AR performance, a simple but robust strategy of partial ambiguity resolution is suggested, where the satellite elevation, number of consecutive tracking, success rate and ratio test are all combined to determine the subset of ambiguity. The DISB results based on zero/ultra-short baseline with different receiver firmware version shows that the code and phase DISB is rather stable over time which means that it could be corrected in advance. Three long baselines range from 570 to 1200 km were tested with DISB calibration in advance to verify the proposed model. The results shows that TC strategy do not improve the value of ratio but shorten the time to reach 100% success rate, compared with the LC strategy. At the same time, TC strategy could significantly shorten the time to first fix and improve the fixing rate of epochs slightly, which means that under some circumstances, LC strategy could only keep float solutions while the TC strategy could still get ambiguity-fixed solutions. In term of positioning accuracy, the precision in up direction is worse than that in north and east direction. Once the ambiguity is fixed correctly, both LC and TC strategy can achieve centimeter-level positioning accuracy. This paper just gives the preliminary research results about the DISB application under long baseline circumstances. Using more data for experimental verification and investigating of what performance the real-time precise products could archive are the points that we will focus on and continue to research.

References

1. Pan SG, Meng X, Wang SL et al (2015) Ambiguity resolution with double troposphere parameter restriction for long range reference stations in NRTK system. Surv Rev 47 (345):429–437
2. Gao W, Gao C, Pan S et al (2015) Improving ambiguity resolution for medium baselines using combined GPS and BDS dual/triple-frequency observations. Sensors 15(11):27525–27542
3. Gao W, Gao C, Pan S et al (2017) Method and assessment of BDS triple-frequency ambiguity resolution for long-baseline network RTK. Adv Space Res
4. Julien O, Alves P, Cannon ME et al (2003) A tightly coupled GPS/GALILEO combination for improved ambiguity resolution. In: Proceedings of the European Navigation Conference (ENC-GNSS'03), pp 1–14
5. Liu H, Shu B, Xu L et al (2017) Accounting for inter-system bias in DGNSS positioning with GPS/GLONASS/BDS/Galileo. J Navig, 1–13
6. Paziewski J, Wielgosz P (2015) Accounting for Galileo–GPS inter-system biases in precise satellite positioning. J Geodesy 89(1):81–93
7. Odijk D, Teunissen PJG (2013) Estimation of differential inter-system biases between the overlapping frequencies of GPS, Galileo, BeiDou and QZSS. In: 4th international colloquium scientific and fundamental aspects of the Galileo programme, pp 4–6
8. Montenbruck O, Hauschild A, Hessels U (2011) Characterization of GPS/GIOVE sensor stations in the CONGO network. GPS Solutions 15(3):193–205
9. Odijk D, Teunissen PJG (2013) Characterization of between-receiver GPS-Galileo inter-system biases and their effect on mixed ambiguity resolution. GPS Solutions 17 (4):521–533
10. Tian Y, Ge M, Neitzel F et al (2017) Particle filter-based estimation of inter-system phase bias for real-time integer ambiguity resolution. GPS Solutions 21(3):949–961
11. Gao W, Gao C, Pan S et al (2017) Inter-system differencing between GPS and BDS for medium-baseline RTK positioning. Remote Sens 9(9):948
12. Mowlam AP, Collier PA (2004) Fast ambiguity resolution performance using partially-fixed multi-GNSS phase observations. In: International symposium on GNSS/GPS. Sydney, Australia, pp 6–8
13. Parkins A (2011) Increasing GNSS RTK availability with a new single-epoch batch partial ambiguity resolution algorithm. GPS Solutions 15(4):391–402
14. Gao W, Gao C, Pan S (2017) A method of GPS/BDS/GLONASS combined RTK positioning for middle-long baseline with partial ambiguity resolution. Surv Rev 49(354):212–220
15. Wang J, Feng Y (2013) Reliability of partial ambiguity fixing with multiple GNSS constellations. J Geodesy, 1–14
16. Brack A (2016) Partial ambiguity resolution for reliable GNSS positioning—a useful tool? In: Aerospace conference, 2016 IEEE. IEEE, pp 1–7

17. Teunissen PJG, Joosten P, Tiberius C (1999) Geometry-free ambiguity success rates in case of partial fixing. In: Proceedings of ION-NTM, pp 25–27
18. Schmid R, Steigenberger P, Gendt G et al (2007) Generation of a consistent absolute phase-center correction model for GPS receiver and satellite antennas. J Geodesy 81(12):781–798
19. Wu JT, Wu SC, Hajj GA et al (1992) Effects of antenna orientation on GPS carrier phase. Astrodynamics 1991, 1647–1660
20. Petit G, Luzum B (2010) IERS conventions. BUREAU INTERNATIONAL DES POIDS ET MESURES SEVRES (FRANCE)